



# Modeling the aeroacoustic noise of large wind energy systems for sound damping control purposes

Andrea Rivarola<sup>1</sup> and Adrian Gambier<sup>2,\*</sup>

<sup>1</sup>National Institute of Industrial Technology, Mendoza, 5507, Argentina

<sup>2</sup>Fraunhofer Gesellschaft, Bremerhaven, 27572, Germany

\*Corresponding author. Email address: agambier@ieee.org.

## Abstract

An important problem for the social acceptance of the wind turbines is the noise that they introduce into the environment, particularly during the night hours in towns close to the wind farms. This problem is normally mitigated by reducing the rotor speed. The control system implementation requires a change in the setpoint of the collective pitch controller. This leads, consequently, to a minor power conversion.

The present contribution uses simple models for noise emission, propagation, and prediction in order to design controllers that mitigate noise with reduced power losses. The parameter tuning problem is solved with a game-theoretic approach and multi-objective optimisation. The simulation results show an increment in the power conversion for the same legal noise limits. Hence, the concept looks promising for applications to real machines.

**Keywords:** Wind turbines; pitch control; acoustic noise reduction; parametric multi-objective optimization

## 1. Introduction

The noise emitted by wind turbines is a clear barrier to the acceptance of wind energy, particularly in the case of onshore installations. For this reason, research regarding noise emission, modelling, measurement, propagation, and reduction has become more and more relevant.

There are several sources that generate acoustic noise in wind turbines. The most important are the mechanical noise, which is studied, e.g., in Hubbard and Shepherd, (1991), and the aerodynamic noise. The mechanical noise can be mitigated in the nacelle (Sørensen, 2012), by using isolation plates (see Barone, 2011) and active damping control of the drive train as presented in Burton et al., (2011). Therefore, the present study is devoted to the modelling of aerodynamic noise for control purposes.

The goal is to find simple models for the emission, propagation, and prediction of aerodynamic noise that may be used to develop control approaches that reduce

the noise of wind turbines that are several hundred metres distant from towns.

Aeroacoustic noise reduction by using control has been investigated, e.g., in Cardenas-Dobson and Asher, (1996) and in Møller and Pedersen, (2011). Some approaches, such as Bertagnolio et al., (2014), Maizi et al., (2017) and Mackowski and Carolus, (2021), utilize control to lower aeroacoustic noise. Moreover, other contributions are dedicated to mitigate the aeroacoustic noise by using the pitch control system. The most common approach consists in switching the setpoint of the collective pitch control to a lower value during the night. Another way is to extend the duties of individual pitch control to attenuate noise, as suggested in Bertagnolio et al., (2014), Maizi et al., (2017) and Mackowski and Carolus, (2021).

However, the induced sound is sensitive to the angle of attack of the blade aerofoils (Oerlemans et al., 2007), which decreases with the increase of the pitch angle. This leads to a contraction in the turbulent boundary layer of the suction side of the airfoils, causing not only noise but also power reduction. Contrarily, reducing the



pitch angle increases the noise and the power extraction. Thus, the permanent pitching activity produces changes in the induced sound all the time. Hence, the pitch control system introduces disturbances into the sound source but is also a means to mitigate them.

The above-mentioned contributions to reducing noise do not consider the trade-off between maximum power extraction and minimal noise emission. Thus, this aspect is also considered in the present work, where the application example considers noise mitigation and power extraction as compromised by using multi-objective optimization following the approach of Gambier (2017), for collective pitch control and tower damping control. Thus, control loops for collective pitch control and noise attenuation are optimally combined.

The rest of the paper is structured as follows: Section 2 is devoted to present the problem description. Simple models for acoustic noise from wind turbines that can be applied for control purposes are described in Section 3. This is complemented with parameter estimation and validation in Section 4. Noise damping control is introduced in Section 5, and the application study is the subject of Section 6. Finally, conclusions are drawn in Section 7.

## 2. Problem description

Onshore wind turbines emit audible aerodynamic noise that spreads geographically to population settlements, typically in rural or semi-rural areas. This noise is particularly annoying and unacceptable during nighttime sleeping hours. The noise generation is a direct consequence of the dynamic rotation and depends mainly on the rotational speed and its variation, which in the full load operation is mainly caused by the pitch activity. Hence, the way to mitigate audible noise is by slowing down the rotation and constraining the pitch speed. The consequence is a power fall.

Since the noise suffers different changes during the travel due to, for example, reflections, absorption, attenuation, and friction, it is not the noise at the emission place that is important but at the place where people suffer the effects (see Figure 1).

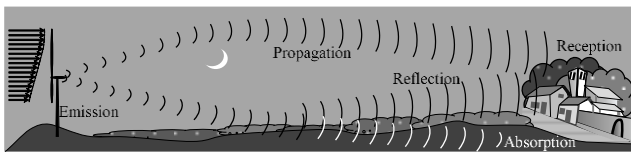


Figure 1. Scheme for the problem description

Aeroacoustic noise can be effectively reduced using the feedback control. This kind of issue can be resolved in two different ways. The first one needs a noise measurement equipment to be installed in the lobby. Nevertheless, this is expensive, both for the necessary measurement equipment and for the transportation of the data back to the control hardware, which is often found inside the wind turbine.

The alternative is to use prediction models. This approach is economically attractive, although the

difficulty lies in the fact that the models are imprecise and, moreover, they require validation and calibration. The objective here consists, therefore, of determining if it is possible to obtain approximate models and a control strategy that provide a noise reduction at the level ordered by the legislation while at the same time minimizing the power drop. The available models are analyzed in the next section.

## 3. Models for the aeroacoustic representation

### 3.1. Prediction models

The specialised literature has reported many noise prediction models. In Lowson, (1992), such models are classified into three groups: Class I corresponds to simple stationary models; models with middle complexity are grouped in Class II; and Class III is reserved for models with complete information on noise processes related to wind turbines. The different models are compared in Zidan et al., (2014). Only a few of them are described in the following.

#### 3.1.1. Sound power level depending on rated power

A very simple model for the sound power level was proposed in Lowson, (1992). This model is given by

$$L_{wA} = 10 \log_{10} P_{wT} + 50. \quad (1)$$

$L_{wA}$  represents the A-weighted sound power level of the emitter, and  $P_{wT}$  is the rated power of the wind turbine in watts.

#### 3.1.2. Sound power level depending on rotor diameter

In Hau et al., (1993), a simple model depending on rotor diameter  $D$  is proposed. The formula is given by

$$L_{wA} = 20 \log_{10} D + 72. \quad (2)$$

#### 3.1.3. Sound power level depending on rotational speed

In Hagg et al., (1992), a model that depends on the tip speed is proposed according to the equation

$$L_{wA} = 50 \log_{10} v_{tip} + 10 \log_{10} D - 4. \quad (3)$$

Since the tip speed of the blade is  $v_{tip} = 0.5 D \omega_r$ , where  $\omega_r$  is the rotor speed, can also be used to describe the tip speed, (3) can be rewritten in dependence on the rotor speed and rotor diameter as

$$\begin{aligned} L_{wA} &= 50 \log_{10} (0.5D \omega_r) + 10 \log_{10} D - 4 \\ &= 50 \log_{10} (\omega_r) + 60 \log_{10} D - 19.0515 \end{aligned} \quad (4)$$

Equation (4) is helpful since the sound power level  $L_{wA}$  depends on the rotor speed  $\omega_r$ , which in turn is reliant on the pitch control system. As a result, (4) can be used in order to express the emission as a function of a space state variable, namely the rotor speed  $\omega_r$ .

It is noted in Wagner et al., (1996), that all these formulas are very imprecise. Therefore, they can be used in particular cases if the parameters are adjusted to satisfy

the measurement data. In the case of real-time control, the prediction can be complemented by sensor data.

### 3.2. Simple Models for the Propagation

The noise of wind turbines is actually a problem at the receiver position. Thus, the emission models have to be complemented by a propagation model. A thorough discussion of propagation models is provided in (Wagner et al., 1996). The idea presented here follows the standard ISO 9613 (ISO-9613, 1993; ISO-9613, 1996).

The sound pressure level that reaches the receiver location can be computed by

$$L_{pA} = L_{wA} + L_{cf} - A, \quad (5)$$

where  $L_{wA}$  has already been defined,  $L_{cf}$  represents a correction factor given in dB (zero for the radiation into free space), and  $A$  is the attenuation in dB that includes different components, as, for example,

$$A = A_{gd} + A_{atm} + A_{gr} + A_{bar} + A_{\sigma}. \quad (6)$$

$A_{gd}$  is the attenuation as a result of the geometric spreading. Hemispherical, spherical, or cylindrical dispersions lead to different values, such as, for instance,

$$\begin{aligned} A_{gd,h} &= 10 \log_{10}(2\pi(d/d_0)^2) = 20 \log_{10}(d/d_0) + 8 \text{dB}, \\ A_{gd,s} &= 10 \log_{10}(4\pi(d/d_0)^2) = 20 \log_{10}(d/d_0) + 11 \text{dB}, \text{ and} \quad (7) \\ A_{gd,c} &= 10 \log_{10}(2\pi(d/d_0)) = 10 \log_{10}(d/d_0) + 8 \text{dB}. \end{aligned}$$

Parameters  $d_0$  and  $d$  represent a reference distance (normally 1 m) and the distance from the emitter to the receiver in meters. The numbers in dB at the end of equations are obtained from  $8 \text{ dB} \approx 10 \log_{10}(2\pi)$  and  $11 \text{ dB} \approx 10 \log_{10}(4\pi)$ . The calculation of the distance  $d$  requires considering the hub height  $h_h$  of the wind turbine and the horizontal distance  $l_d$  to the receiver, and it is expressed by

$$d = \sqrt{l_d^2 + h_h^2}. \quad (8)$$

For the atmospheric attenuation  $A_{atm}$ , a very simple equation given by

$$A_{atm} = \alpha d \quad (9)$$

is used, where  $\alpha$  is the atmospheric absorption in dB/m. It is a function of frequency, temperature, humidity, and pressure.

Further components that can be added to the attenuation equation are, for example, ground absorption ( $A_{gr}$ ), screening ( $A_{bar}$ ), as well as, according to Lovtidende, (2017), the sound insulation  $A_{\sigma}$ .

Factors  $A_{gr}$ ,  $A_{\sigma}$ , and  $\alpha$  depend on the frequency, and therefore, they are commonly described for each fundamental frequency of the 1/3-octave bands, as described in Lovtidende, (2017). Hence, equation (5) is applied for each band. The total sound pressure level is computed by using

$$L_{pA,tot} = 10 \log_{10} \left( \sum_{i=1}^n 10^{L_{pA}^{(i)}/10} \right). \quad (10)$$

In the downwind direction and for distances closer to the wind turbine, the spread can be assumed to be spherical. Hence, the A-weighted sound pressure level (SPL) is characterized by the fact that the sound pressure level attenuates 6 dB per distance doubling (see Møller and Pedersen, (2011)), is given by

$$L_{pA} = L_{wA} - 20 \log_{10}(d/d_0) - \alpha d - 11 \text{ dB}, \quad (11)$$

where a typical value for  $\alpha$ , according to Rogers et al., (2006), is 0.005 dB/m.

According to Hubbard and Shepherd, (1991), the propagation for distances larger than 200 m verifies a cylindrical spread, and the attenuation decreases by around 3 dB for every doubled distance. The model has been proposed by Møller and Pedersen, (2011), and the equation is

$$L_{pA} = L_{wA} - 20 \log_{10}(200\text{m}/1\text{m}) - 10 \log_{10}(d/200\text{m}) - \alpha d - 11 \text{ dB} + A_g, \quad (12)$$

where  $A_g$  is a ground effect correction, whose values are 1.5 dB for onshore and 3 dB for offshore wind turbines. The Danish standard (e.g., Lovtidende, 2017) suggests a propagation formula for low-frequency noise that responds to

$$L_{pA} = L_{wA} - 10 \log_{10}(h_h^2 + d^2) - \alpha \sqrt{h_h^2 + d^2} - A_{\sigma} - A_{glLF} - 11 \text{ dB} + A_g. \quad (13)$$

$\Delta L_{glLF}$ , and  $\Delta L_{\sigma}$  denote the ground effect and sound isolation at low frequencies, respectively.

### 3.3. Modelling the background acoustic noise

According to Fitzell and Phil, (2019), background acoustic noise levels ranged from roughly 30 dB(A) in rural and suburban areas to more than 120 dB(A) in urban and commercial locations. It is pointed out in Hansen and Hansen, (2020), that level swings between 30 and 48 dB(A) can be assumed.

On the other hand, the interaction between wind and foliage in rural areas has been studied by Fégeant, (1999). It could be verified that this interaction is nearly proportional to the base 10 logarithm of the wind speed. In other words,

$$L_{pAwind} = K_1 \log_{10}(K_2 v_w) + K_3. \quad (14)$$

Finally, Rogers et al., (2006) pointed out that the wind itself causes background noise that ranges from 25 dB(A) (in calm conditions) to 42 dB(A).

## 4. Parameter estimation and model validation

The important models to be adjusted and validated are those defined by equations (4) and (14) because they depend on other variables related to the wind turbine. Equation (14) is now rewritten in a more abstract way in order to be able to adjust it to the available data, namely

$$L_{wA} = a \log_{10}(bD \omega_r + c) + d \log_{10}(eD) + f. \quad (15)$$

Given the variables  $v_w$ ,  $\omega_r$ ,  $L_{p\omega}$ , and  $L_{pA_{wind}}$  from real data, as well as the rotor diameter  $D = 126$  m, the unknown parameters  $a, b, c, d, e, f, K_1, K_2$ , and  $K_3$  are estimated to fit (14) and (15). To this end, the nonlinear least squares method with the trust-region algorithm is used. The result is shown in Figure 2.

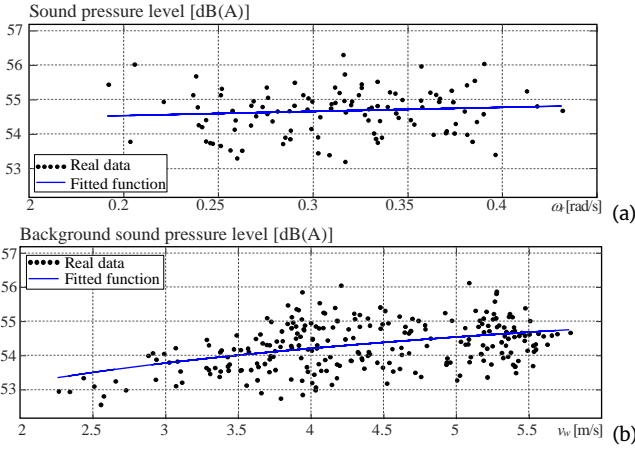


Figure 2. Fitted functions for equations (14) (a), and (15) (b)

The obtained parameters are summarized in Table 1.

Table 1. Parameters for equations (14) and (15)

Equation	Parameters	Values
(14)	$a$	5.51348
	$b$	1.17689
	$c$	25.61593
	$d$	1.512282
	$e$	-5.84898
	$f$	1.96914
(15)	$K_1$	3.42450
	$K_2$	13.10747
	$K_3$	48.32280

The real data used to find the parameters presents important dispersion, but in a reduced range of 5 dB, as can be observed in Figure 2. Therefore, the obtained parameters lead to equations that work as averaging functions. Hence, the RMSE shows acceptable values, but the R-square values are too low. However, the estimated functions provide a satisfactory approximation for the control duty as shown in the numerical study. The goodness of fit statistics is summarized in Table 2.

Table 2. Goodness of fit Statistics for equations (14) and (15)

Equation	Parameters	Values
(14)	SSE	41.337
	RMSE	0.63661
	R-squared	0.0089
(15)	SSE	99.03
	RMSE	0.6306
	R-squared	0.1774

## 5. Application to noise damping control

The aim of the models discussed in the preceding sections is their application for control purposes. The application chosen for the present study is to reduce the wind turbine noise level near settlements to the legal threshold value while still maximizing energy conversion. In particular, the requirement is important during the night in full-load operation under active pitch control.

### 5.1. Operational regions and control strategies

Large wind turbines have an operation characterized by regions that depend on the wind speed (see, e.g., Bianchi et al., (2007), Gambier, (2022), Burton et al., (2011)). This is described in Figure 3.

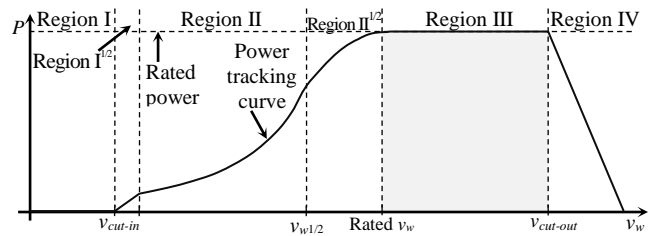


Figure 3. Operational regions of a wind turbine (see, e.g., Gambier, (2022))

The wind turbine is operated in Region I, where it revolves freely without converting energy if the wind speed  $v_w$  is below the cut-in value. Once the wind speed exceeds the cut-in threshold and the transition ends, the machine enters Region II, also known as the partial load operational region, and remains there as long as the nominal value of  $v_w$  is not reached. Here, the control objective is to maximize the energy conversion. If the wind speed overshoots the nominal value the wind turbine goes after a transient in the full-load operation (Region III) and the control objective is to limit the rotational speed by pitching the blades. If  $v_w$  overdoes the cut-out limit, the machine has to be shut down. The transitions between regions are sometimes referred to as Regions  $I^{1/2}$  and  $II^{1/2}$ , respectively.

### 5.2. Pitch control

The active sound damping control proposed here is limited to the operation in Region III, i.e., a collective pitch control (CPC) system as shown in Figure 4, because the strong wind in this region makes the machine the noisiest.

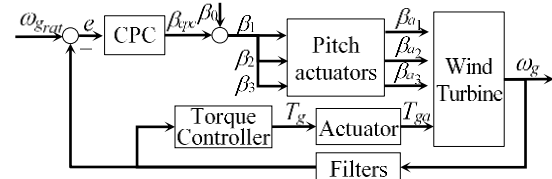


Figure 4. Control system for Region III

The CPC corresponds to a proportional-integral (PI) control law with gain scheduling. The PI controller is formulated in the Laplace domain by

$$G_{PI}(s) = K_p + \frac{K_i}{s} = \frac{K_i + K_p s}{s}, \quad (16)$$

where  $K_p$  and  $K_i$  are the controller gains and are computed from

$$K_p = \frac{K_p^o}{\partial P / \partial \beta |_{\beta_0}} \text{ and } K_i = \frac{K_i^o}{\partial P / \partial \beta |_{\beta_0}} \quad (17)$$

with  $P$  as power. Parameters  $K_p^o$  and  $K_i^o$  are obtained by optimization for the operation at rated values. By changing the wind speed, the operating point as well as the pitch angle  $\beta_0$  also change. Hence, the sensibility function  $\partial P / \partial \beta |_{\beta_0}$  is used as a scheduling parameter to adjust the controller gains accordingly.

### 5.3. Active sound damping control

The concept proposed here is to restrict the pitch control loop to a cascaded external control loop. The outer control loop has as its setpoint the legal limit for the noise level. As a feedback variable, the generator speed is taken, which is used to estimate the noise level propagated to the village and to which the background noise is added. This control loop gives a setpoint for the CPC, which is the maximum that can be targeted for the current legal noise level. This setpoint is dynamically adjusted according to the value of the background noise present at any given moment.

Thus, the idea is to implement a tracking control system such that the power conversion takes place adaptively in order to maximize power while maintaining the sound threshold below the limit. This is called active sound damping control (ASDC) and its configuration is shown in Figure 5.

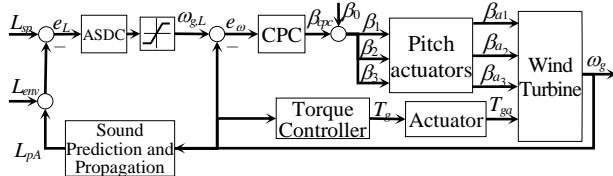


Figure 5. Control system in cascade configuration including CPC and ASDC

The saturation block ensures that the setpoint for the generator speed does not exceed the maximum value when the sound level pressure is very low. The highest value in the saturation block is set to the rated generator rotational speed.

### 5.4. Parameter tuning by using multi-objective optimization

The parameter tuning of a multi-loop control system with several controllers follows the methodology proposed in Gambier, (2017), Gambier and Nazarrudin, (2018), Gambier et al., (2006). The controllers of a coupled multi-loop control system are players in a nonzero-sum cooperative dynamic game (see Haurie, (2001), Petrosjan, (2005), Schmitendorf, (1972). Each player receives an objective function (payoff) such that all together

they constitute a vector-valued objective function.

$$\mathbf{J} = [J_1 \ J_2 \ \dots \ J_m]^T. \quad (18)$$

The solution is obtained by using a multi-objective optimization algorithm that delivers a Pareto front, as shown in Figure 6. Each point on the Pareto front is an equally optimal solution. Hence, a decision maker is applied to find a unique final solution.

Decision-making can be based on different procedures. The most common is the compromise solution (CS). However, bargaining games provide other ways, as for instance, the Nash solution (NS), the Kalai-Smorodinsky solution (KS) and the egalitarian solution (ES). All are described in Figure 6.

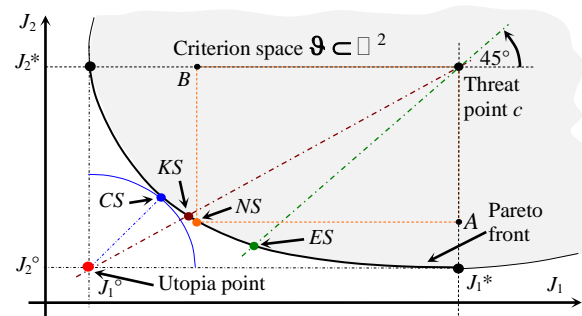


Figure 6. Decision maker using bargaining games

## 6. Simulation Study

### 6.1. Scenario and simulation setup

The NREL 5MW wind turbine with an onshore setting is used for the numerical study (Jonkman et al., 2009). It has a rotor with a diameter of 126 m, where the blades are 61.5 m long, and the 3m-diameter hub is located at a height of 90 m (see Figure 7).

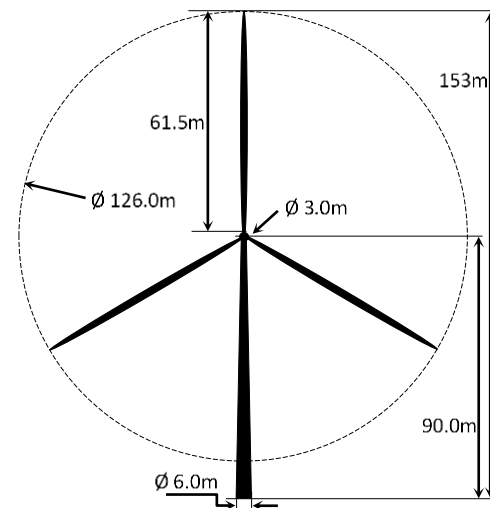


Figure 7. Scheme of the NREL 5MW wind turbine

The generator efficiency is rated to 94.4%, such that mechanical power is 5.30 MW. An optimum tip-speed

ratio of 7.55 results in the highest power factor  $C_p$  of 0.482. The rated rotor speed is 12.1 rpm for a wind speed of 11.4 m/s, and it is connected to the generator through a gearbox with a ratio of 97:1. Hence, the rated generator speed is 1173.7 rpm. Since the cut-in rotor speed is 6.9 rpm, the noise emission computed by using (4) ranges from 99.4 to 112.1 dB(A). The rated values are summarized in Table 3.

Table 3. Rated values of the 5 MW reference wind turbine

Rated variables	Values
Rated mechanical power	5.30 MW
Rated rotor speed	12.1 rpm
Cut-in and rated wind speed	6.9 rpm, 11.4 m/s
Peak power coefficient, optimal TSR	0.482, 7.55

The receiver is 400 meters from the wind turbine, and the sound attenuation caused by aerial, ground, and environmental factors is 58.7 dB(A). For small populated areas, the German law permits a maximum daytime noise level of 55 dB(A) and a nighttime noise level of 40 dB(A). These aeroacoustic conditions are summarized in Table 4.

Table 4. Aeroacoustic values for the simulation scenario

Simulation scenario	Values
Distance to receiver	400 m
Aerial-ground attenuation	58.7 dB(A)
Legal level (day, night)	55 dB(A), 40 dB(A)
Noise emission range	99.4 – 112.1 dB(A)

The operation takes place in Region III with an effective wind speed changing between 11.5 and 20 m/s, including tower shadow and turbulence of 10%, for 30 minutes.

### 6.2. Control system design

The control system design consists of finding the parameters of the controllers of both coupled control loops. The joint tuning of all parameters is carried out by using the approach proposed in Gambier et al., (2006) and the bat algorithm described in Gambier and Nazaruddin, (2022).

As objective functions to be optimized, the time-averaged performance indices

$$J_\omega = \frac{1}{t_f - t_0} \int_{t_0}^{t_f} t e_\omega^2 dt \text{ and } J_L = \frac{1}{t_f - t_0} \int_{t_0}^{t_f} t e_L^2 dt. \quad (19)$$

are used, where  $e_\omega$  and  $e_L$  are the control errors of both control loops. The numerical optimization requires the evaluation of the objective functions at every iteration. Thus, a simulation-based procedure is applied, where the evaluations are obtained numerically as part of the simulation, as shown in the scheme of Figure 8. Since the evaluations are limited to a finite period of time, the performance indices must be averaged over time.

Wind turbines also have actuators, which have limited output ranges. This aspect has to be included in the optimization process. For example, pitch actuators are limited in rotation angle and in rate, namely

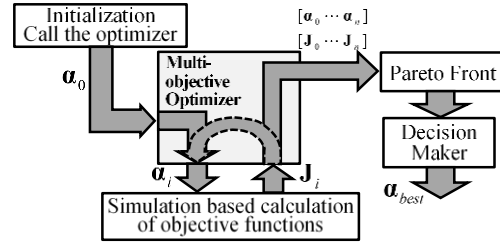


Figure 8. Simulation-based multiobjective optimization scheme

$$\beta_{\min} \leq \beta \leq \beta_{\max} \text{ and } \dot{\beta}_{\min} \leq \dot{\beta} \leq \dot{\beta}_{\max}. \quad (20)$$

Moreover, the control signal of the ASDC is limited because it is the setpoint for the CPC, i.e.,

$$\omega_{g,\text{cut-in}} \leq \omega_{gL} \leq \omega_{g,\text{rated}}. \quad (21)$$

For the present study, these limits are given in Table 5 following common values of real pitch actuators.

Table 5. Limit values for the controller outputs

Rated variables	Angle/Speed	Rate
Minimum value (pitch)	0 deg	-8 deg/s
Maximum value (pitch)	25 deg	+8 deg/s
Minimum value (sound)	6.9 rpm	----
Maximum value (sound)	12.1 rpm	----

The multiobjective optimizer delivers the Pareto front of Figure 9.

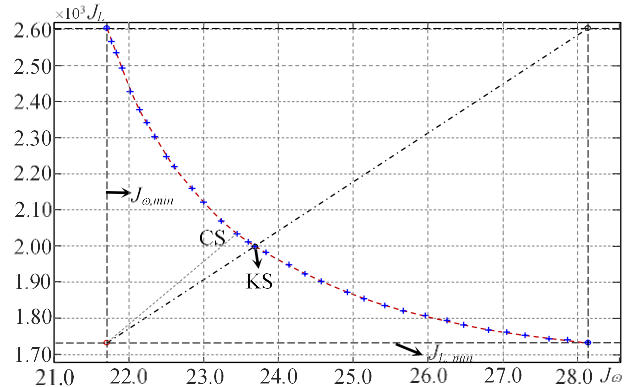


Figure 9. Pareto front for ( $J_\omega$  vs.  $J_L$ )

The Kalai-Smorodinsky solution in the objective space is  $(J_\omega, J_L) = (23.8, 1.99 \times 10^3)$ , and the solution in the parameter space is summarized in the right column of Table 6.

Table 6. Controller Parameters

Gains	Classic Approach	Cascade Approach
$K_{pL}$	--	-1.38290
$K_{iL}$	--	-0.00084
$K_{aL}$	--	0.5
$K_{p\omega}$	1.51	1.64078
$K_{i\omega}$	0.653	0.56139
$K_{a\omega}$	8.0	0.5

### 6.3. Simulation Results and Analysis

In order to evaluate the results, the classic approach is also considered. The classic approach is very simple: during the night, the setpoint of the CPC is set to a value that guarantees the noise level limit in the worst case, i.e., independently of background noise. In the current case, this is given at 7.65 rpm. In addition, an intermediate case (flexibilized classic approach) with a value of 8.0 rpm has been defined. This case provides more energy under the premise that the noise level can be a little bit higher.

The simulation is set to begin four minutes before entering nighttime, and then it is switched to nighttime operation. The complete simulation lasts 30 minutes. The results are shown in Figure 10.

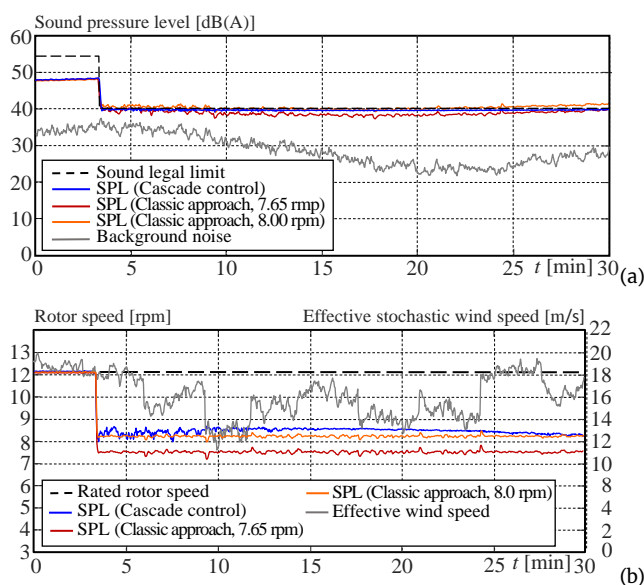


Figure 10. Simulation results for the classic approach. (a) SPL. (b) Rotor speed.

Since the SPL does not reach the legal level of 55 dB (A) for the rated rotor speed during the day, no power restriction is necessary. It is also observed that the cascade control system maintains the legal limit during night operation while maximizing the rotor speed. This is not possible to obtain with the classic approach, which always maintains a constant rotor speed even when the sound level would allow a higher value.

The above-described aspects regarding the rotor speed have a quantitative correlate in the power conversion. To this end, a quantitative performance comparison is carried out by using the converted energy during the simulation time in kWh. The results are summarized in Table 7.

Table 7. Energy converted by the different approaches in 30 minutes

	Energy in kWh	
	Setpoint 7.65 rpm	Setpoint 8.0 rpm
Classic Approach	4262.84	4456.67
Cascade Approach	4485.61	

Assuming an operation of 8 hours per day and 365 days in a year with similar wind conditions and 8 eurocent per kWh, the use of the cascade approach, against the classic approach, would produce a win per wind turbine of 13,000 € for the setpoint at 7.65 rpm and 1,6090 € if the setpoint is 8.0 rpm.

### 7. Conclusions

In this work, models for the emission, propagation, and prediction of aeroacoustic noise from wind turbines and their application to control system design are presented. An application example is described. It included a second control loop in a cascade configuration, whose setpoint is the allowed noise level limit.

By using multi-controller design based on multiobjective optimization, it is possible to find a dynamic compromise between the legal noise limit and maximum power conversion for the current conditions.

Very satisfactory simulation results are obtained. Such that a promising real-time application can be expected. The next steps in the research are to consider more sophisticated models and the control system implementation in a real-time simulation environment.

### Funding

This work has been financed by the Federal Ministry of Economic Affairs and Climate Action (BMWK).

### References

- Barone, M. F. (2011). Survey of techniques for reduction of wind turbine blade trailing edge noise, Research report, Wind Energy Technology, Sandia National Laboratories, SAND2011-5252, Sandia National Laboratories, Albuquerque.
- Bertagnolio, F., Aagaard Madsen, H., Fischer, A. and Bak, C. (2014). Cyclic pitch for the control of wind turbine noise amplitude modulation. Proceedings of the *Inter-noise 2014*, Melbourne, 1 – 8, 16 – 19 November 2014.
- Bianchi, F. D., de Battista, H. and Mantz, R. J. (2007). *Wind Turbine Control Systems*, Springer Nature, London, UK.
- Burton, T., Jenkins, N., Sharpe, D. and Bossanyi, E. (2011). *Wind Energy Handbook*, 2nd edn, John Wiley & Sons, Chichester, UK.
- Cardenas-Dobson, R. and Asher, G. M. (1996). Power limitation in variable speed wind turbines using pitch control and a mechanical observer. *Wind Engineering*, 20: 363 – 387.
- Fégeant, O. (1999). On the masking of wind turbine noise by ambient noise. Proceedings of the *European Wind Energy Conference*, Nice, France, 184 – 188, 1–5 March 1999.
- Fitzell, R. and Phil, M. (2019). Expected ambient noise levels in different land-use areas. Proceedings of the

- Acoustics 2019*, Cape Schanck, Australia, 1 – 10, 10–13 November 2019.
- Gambier, A. (2017). Simultaneous design of pitch control and active tower damping by using multi-objective optimization. Proceedings of the *1st IEEE Conference on Control Technology and Applications*, Kohala Cost, USA, 1679 – 1684, 17–20 December 2017.
- Gambier, A. (2022). *Control of Large Wind Energy Systems*, Springer Nature, Basel, Switzerland.
- Gambier, A. and Nazaruddin, Y. (2022). Wind turbine pitch and active tower damping control using metaheuristic multi-objective bat optimization. Proceedings of the *19th International Multidisciplinary Modeling & Simulation Multiconference*, Rome, 1 – 9, 19–21 September 2022.
- Gambier, A., Wellenreuther, A. and Badreddin, E. (2006). A new approach to design multi-loop control systems with multiple controllers. Proceedings of the *45th IEEE Conference on Decision and Control*, San Diego, USA, 1828 – 1833, 13–15 December 2006.
- Hagg, F., van der Borg, N. J. C. B., C., J. and al., e. (1992). Definite Aero-Geluidonderzoek Twin, SPE 92-025, Stork Product Engineering B. V.
- Hansen, C. and Hansen, K. (2020). Recent advances in wind turbine noise research. *Acoustics*, 2: 171 – 206.
- Hau, E., Langenbrinck, J. and Palz, W. (1993). *WEGA Large Wind Turbines*, Springer-Verlag, Berlin.
- Hubbard, H. H. and Shepherd, K. P. (1991). Aeroacoustics of large wind turbines. *Journal of the Acoustic Society of America*, 89: 2495 – 2508.
- Jonkman, J., Butterfield, S., Musial, W. and Scot, G. (2009). *Definition of a 5-MW Reference Wind Turbine for Offshore System Development*, NREL, Golden, Colorado, USA.
- Lovtidende (2017). Statutory Order on noise from wind turbines, Gazette, Danish Environmental Protection Agency.
- Lowson, M. V. (1992). Assessment and prediction of wind turbine noise, Research report, Flow Solutions Ltd., ETSU-W--13/00284/REP, Bristol, UK.
- Mackowski, L. and Carolus, T. H. (2021). Wind turbine trailing edge noise: mitigation of normal amplitude modulation by individual blade pitch control. *Journal of Sound and Vibration*, 510: 116279.
- Maizi, M., Dizene, R. and Mihoubi, M. C. (2017). Reducing noise generated from a wind turbine blade by using pitch angle control using CFD and acoustic analogy. *Journal of Applied Fluid Mechanics*, 10: 1201 – 1209.
- Møller, H. and Pedersen, C. S. (2011). Low-frequency noise from large wind turbines. *Journal of the Acoustic Society of America*, 129: 3727 – 3744.
- Rogers, A. L., Manwell, J. F. and Wright, S. (2006). Wind turbine acoustic noise, White paper, Mechanical and Industrial Engineering, University of Massachusetts, University of Massachusetts, Amherst.
- Schmitendorf, W. E. (1972). Cooperative games and vector-valued criteria problems. Proceedings of the *IEEE Conference on Decision and Control*, vol. 18, New Orleans, USA, 340 – 344, 13–15 December 1972.
- Wagner, S., Bareib, R. and Guidati, G. (1996). *Wind Turbine Noise*, Springer Verlag, Berlin, Germany.
- Zidan, E., Elnady, T. and Elsabbagh, A. (2014). Comparison of sound power prediction models of wind turbines. Proceedings of the *International Conference on Advances in Agricultural, Biological & Environmental Sciences*, Dubai, UAE, 49 – 54, 15–16 October 2014.